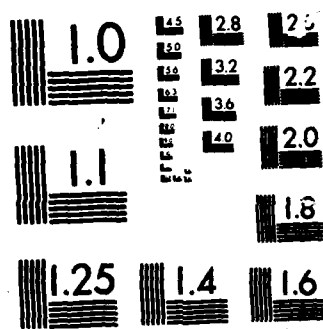


RD-A165 737 CHARACTERIZATION OF SPUTTER DEPOSITED Al-NITRIDE AND 1/1  
Al-OXIDE BY X-RAY PH. (U) WISCONSIN UNIV-MADISON  
C J KUBIAK ET AL. 1986 ARO-21334.5-MS DAAG29-84-K-0126  
UNCLASSIFIED F/G 7/4 NL



MICROCOPY RESOLUTION TEST CHART  
NATIONAL BUREAU OF STANDARDS 1963-A

AD-A165 737

UNCLASSIFIED

SECURITY CLASSIFICATION OF THIS PAGE (When Data Entered)

2

REPORT DOCUMENTATION PAGE		READ INSTRUCTIONS BEFORE COMPLETING FORM
1. REPORT NUMBER ARO 21334.5-MS	2. GOVT ACCESSION NO. N/A	3. RECIPIENT'S CATALOG NUMBER N/A
4. TITLE (and Subtitle) Characterization of Sputter Deposited Al-Nitride and Al-Oxide by X-Ray Photoelectron Loss Spectroscopy		5. TYPE OF REPORT & PERIOD COVERED reprint
7. AUTHOR(s) Charlene J. G. Kubiak, Carolyn Rubin Aita Ngoc C. Tran, Tery L. Barr		6. PERFORMING ORG. REPORT NUMBER DAAG29-84-K-0126
8. PERFORMING ORGANIZATION NAME AND ADDRESS Univ. of Wisconsin		10. PROGRAM ELEMENT, PROJECT, TASK AREA & WORK UNIT NUMBERS
9. CONTROLLING OFFICE NAME AND ADDRESS U. S. Army Research Office Post Office Box 12211 Research Triangle Park, NC 27709		12. REPORT DATE
11. MONITORING AGENCY NAME & ADDRESS (if different from Controlling Office)		13. NUMBER OF PAGES
		15. SECURITY CLASS. (of this report) Unclassified
		16a. DECLASSIFICATION/DOWNGRADING SCHEDULE
16. DISTRIBUTION STATEMENT (of this Report) Approved for public release; distribution unlimited.		
17. DISTRIBUTION STATEMENT (of the abstract entered in Block 20, if different from Report) NA		
18. SUPPLEMENTARY NOTES The view, opinions, and/or findings contained in this report are those of the author(s) and should not be construed as an official Department of the Army position, policy, or decision, unless so designated by other documentation.		
19. KEY WORDS (Continue on reverse side if necessary and identify by block number)		
20. ABSTRACT (Continue on reverse side if necessary and identify by block number) ABSTRACT ON REPRINT		

DTIC FILE COPY

DD FORM 1 JAN 73 1473

EDITION OF 1 NOV 68 IS OBSOLETE

UNCLASSIFIED

SECURITY CLASSIFICATION OF THIS PAGE (When Data Entered)

CHARACTERIZATION OF SPUTTER DEPOSITED Al-NITRIDE AND Al-OXIDE BY  
X-RAY PHOTOELECTRON LOSS SPECTROSCOPYCHARLENE J. G. KUBIAK,\* CAROLYN RUBIN AITA,\* NGOC C. TRAN,\*\* AND  
TERY L. BARR\*\* Materials Department and the Laboratory for Surface Studies  
University of Wisconsin-Milwaukee, P. O. Box 784, Milwaukee, WI 53201\*\*Materials Science Center  
University of Wisconsin-Madison, Madison, WI 53706

## ABSTRACT

*alpha**Delta E*

The results of an x-ray photoelectron loss spectroscopy (XPLS) study of several wide band gap aluminum compounds are presented here. XPLS is a new application of x-ray photoelectron spectroscopy involving the determination of the energy separation,  $\Delta E$ , between a particular core photoelectron peak and its principal loss peak. The materials investigated here are sputter deposited thin film Al-nitride and oxide, and bulk single crystal  $\alpha$ -alumina. It is not possible to distinguish between these materials on the basis of the chemical shift in the binding energy of the Al2p and Al2s photoelectrons (Siegbahn shift). The results show that XPLS can be used to distinguish between these materials.  $\Delta E$  in Al-oxides and nitride differs by several eV and is independent of sample charging. Comparison with  $\Delta E$  calculated using a free electron gas model is made and related to the plasmon nature of  $\Delta E$ .

## INTRODUCTION

Thin films of Al-nitride can be grown near room temperature by reactive sputter deposition. However, oxygen-bearing contaminants in the sputtering discharge seriously affect film crystallinity and optical behavior [1]. Sometimes an oxide [1] or oxynitride [2] second phase is formed. It is difficult to distinguish between Al-nitride and Al-oxide using traditional x-ray photoelectron spectroscopy on the basis of the chemical shift in the Al core electron binding energy because:

1. The Al2p and Al2s electron binding energy for several Al-oxide polymorphs overlap that for Al-nitride.
2. The apparent shift in binding energy due to sample charging is usually greater than the Siegbahn chemical shift. In an attempt to correct for charging, referencing to the C1s XPS peak of adventitious carbon is frequently used. However, this technique is not always reliable. Furthermore, adventitious carbon may be removed upon depth profiling the sample by sputter etching.

In theory, it is possible to distinguish between Al-nitride and Al-oxide on the basis of the existence of an N1s spectrum and the absence of an O1s spectrum different from that for O physisorbed on AlN. However, all three elements are present in many technologically interesting systems and measurement of the O1s binding energy encounters the same problems mentioned above with respect to the Al2p and Al2s photoelectron spectra.

The loss peak is generated by the inelastic interaction of the ejected core photoelectron or its corresponding hole with the sea of valence band electrons [3-5]. For the case of harmonic oscillations of the valence band electrons in a simple metal (plasmons) in which there is no electron localization in the valence band or core electron polarization,  $\Delta E$  is given by the free electron gas expression [6]:

$$\Delta E = \hbar [4\pi e^2 n/m]^{1/2} \quad (1)$$

where  $e$  is the charge on an electron,  $n$  is the density of valence band electrons, and  $m$  is the mass of an electron.

Even for wide band gap materials, loss peaks represent collective transitions if there is sufficient valence band electron delocalization [7,8]. However, part of the valence band electron density may behave in a non-collective manner. These localized states may perturb  $\Delta E$  above or below the free electron gas value, and cause dispersion in the values of  $\Delta E$  associated with photoelectrons originating from different energy states [4,5].

XPLS is easy to instrument. The technique can be carried out on a conventional ESCA system. However, a critical difference between XPLS and other more difficult-to-instrument electron energy loss spectroscopies, EELS for example, is that in XPLS, the measurement is made in the relaxed hole ion system, the final state. Theoretical arguments show that for many materials systems, the value of  $\Delta E$  is independent of relaxation effects [3-5]. If this is the case, then XPLS yields information about the initial chemical state of the material.

With respect to Al-N and Al-O compounds, the purpose of the present study is to answer three questions:

1. Can these materials be distinguished on the basis of different values of  $\Delta E$ ?
2. Is  $\Delta E$  independent of sample charging?
3. Do loss features represent collective transitions of the valence band electrons? To determine this, the values of  $\Delta E$  obtained by XPLS will be compared with theoretical calculations using a free electron gas model.

## EXPERIMENTAL PROCEDURE

A Perkin-Elmer Physical Electronics Model 548 AES/ESCA system was used to take high resolution spectra of the Al2p and Al2s principal XPS peaks using an analyzer energy of 50 eV, and their companion loss peaks using an analyzer energy of 100 eV. Mg  $ka$  x-ray radiation was used. A gold standard was used to calibrate the position of the Au4f<sub>7/2</sub> peak at 83.8 eV, measured to an accuracy of  $\pm 0.2$  eV. Depth profiling of the samples for times up to 300 sec using a 100 eV, 10 ma, Ar<sup>+</sup> ion beam was carried out. The sputtering rate for the materials examined here was estimated to be between 0.3 and 0.5 Å/sec. Depth profiling is used to obtain chemical information from layers below the film surface. The reader is reminded, however, that sputter etching may damage the film surface, and produce artifacts not representative of film chemistry [9].

The following materials were examined:

1. Bulk single crystal (0001)-cut  $\alpha$ -alumina. Data were collected from three samples.

2. Thin film alumina grown by sputter deposition on water-cooled Si-(111) substrates using an Al target and an rf-excited oxygen discharge operated at 600 W rf forward power. Data were collected from three samples. The films showed no x-ray diffraction peaks, indicating that there was no long range crystallographic order. These films are referred to here as "amorphous" or " $\alpha$ -alumina".

3. Thin film Al-nitride grown by reactive sputter deposition on water cooled Si-(111) substrates using an Al target and an rf-excited nitrogen discharge operated at rf forward power levels from 300 to 800 W. The films were found to be Al-rich [1]. Partial oxidation of the excess Al occurred upon exposure to air. The single x-ray diffraction peak from the films was attributable to the (0001) planes of the wurtzite-type AlN lattice. No N-O bonding [2] was detected by XPS.

The chemical composition of the Al-nitride films, obtained from the relative intensity of the Al2p, N1s, and O1s XPS peaks multiplied by the

appropriate sensitivity factor [10] is recorded in Table I. To observe the effects of room temperature aging [1], data was taken from films 5 and 350 days after deposition. It should be noted that although the O content in the films increases in time, the N/Al ratio does not change significantly. This result indicates that O is not replacing N in the films during the aging process.

## RESULTS

A typical loss spectrum, in this case associated with the Al2p photo-electron in Al-nitride, is shown in Fig. 1. To compare the value of  $\Delta E$  generated by photoelectrons from different energy states in the same material,  $\Delta E(\text{Al2p})$  and  $\Delta E(\text{Al2s})$  are shown as a function of the sputter etch time for individual Al-nitride films in Fig. 2, and for  $\alpha$ -alumina and  $\alpha$ -alumina in Fig. 3.

It can be seen from Fig. 2 that within experimental error ( $\pm 0.4$  eV), the value of  $\Delta E$  is independent of whether the loss spectrum was induced by an Al2p or Al2s electron. In contrast, there is pronounced dispersion in  $\Delta E$  associated with Al2p and Al2s photoelectrons in  $\alpha$ -alumina, as can be seen from Fig. 3a. In the case of  $\alpha$ -alumina (Fig. 3b), the data presented here is inconclusive with respect to  $\Delta E(\text{Al2p})$ - $\Delta E(\text{Al2s})$  dispersion. Although the values for  $\Delta E(\text{Al2p})$  consistently lie above those for  $\Delta E(\text{Al2s})$ , they are still within experimental error of each other.

To compare the behavior of  $\Delta E$  associated with photoelectrons from the same energy state in Al-nitride and oxide,  $\Delta E(\text{Al2p})$  and  $\Delta E(\text{Al2s})$  are shown in Figs. 4a and 4b versus sputter etching time for all samples. It can be seen that nitrides and oxides are clearly distinguishable (by several eV) on the basis of both  $\Delta E(\text{Al2p})$  and  $\Delta E(\text{Al2s})$ . However, Al-nitride films having different amounts of incorporated O cannot be differentiated on the basis of  $\Delta E$ .

In  $\alpha$ -alumina, there is no systematic change greater than experimental uncertainty in either  $\Delta E(\text{Al2p})$  or  $\Delta E(\text{Al2s})$  with sputter etching. However, in  $\alpha$ -alumina and Al-nitride, there is a small decrease in  $\Delta E$  with sputter etching. The reason for this decrease is, at present, not clear. One possible explanation is based on the relative stability of octahedral (more stable) and tetrahedral (less stable) bonds in binary systems which contain a common metal cation. In  $\alpha$ -alumina, Al is in 6-fold coordination with O, with Al occupying 2/3 of the octahedral interstices in the close-packed hexagonal O sublattice [11]. In Al-nitride, Al is in 4-fold coordination with N, with Al occupying 1/2 of the tetrahedral interstices in the close-packed hexagonal N sublattice [12]. The average coordination number of Al with O in  $\alpha$ -alumina lies between 4 and 6 [13-15]. A chemical etching study [16], however, showed that in order to relieve surface strain (to decrease the number of dangling bonds), a larger number of Al atoms are in 6-fold coordination at the surface of the material than in the interior. It is possible that this change in Al coordination number in  $\alpha$ -alumina causes the abrupt decrease in  $\Delta E$  from a value identical with  $\alpha$ -alumina at the film surface to a lower value after a 5 sec sputter etch.

Figure 5 shows  $\Delta E(\text{Al2p})$  versus the Al2p principal XPS peak energy in all samples in which charge referencing to the C1s peak at 284.6 eV was possible. It can be seen that although the Al2p principal peak energy overlaps for the Al-nitride and oxides studied here,  $\Delta E(\text{Al2p})$  for each set of compounds is clearly distinguishable.

To demonstrate that  $\Delta E$  is independent of sample charging, Fig. 6 shows  $\Delta E(\text{Al2p})$  versus the Al2p principal peak energy before correction for charging was made. It can also be seen from Fig. 6 that the shift in

TABLE I: Change in Chemistry of Al-Nitride Films with Deposition Discharge Power, Depth Profiling, and Room Temperature Aging

Power (W)	Al:N:O Atomic Ratio		
	0 sec etch	5 sec etch	120 sec etch
300	*10:6:4 +10:4:13	10:5:5 10:4:11	10:6:- 10:5:5
500	+10:6:10	10:6:7	10:7:7
700	+10:7:9	10:6:9	10:8:8
800	*10:8:2 +10:7:9	- 10:9:6	-

Data taken (\*) 5 days and (+) 350 days after deposition.

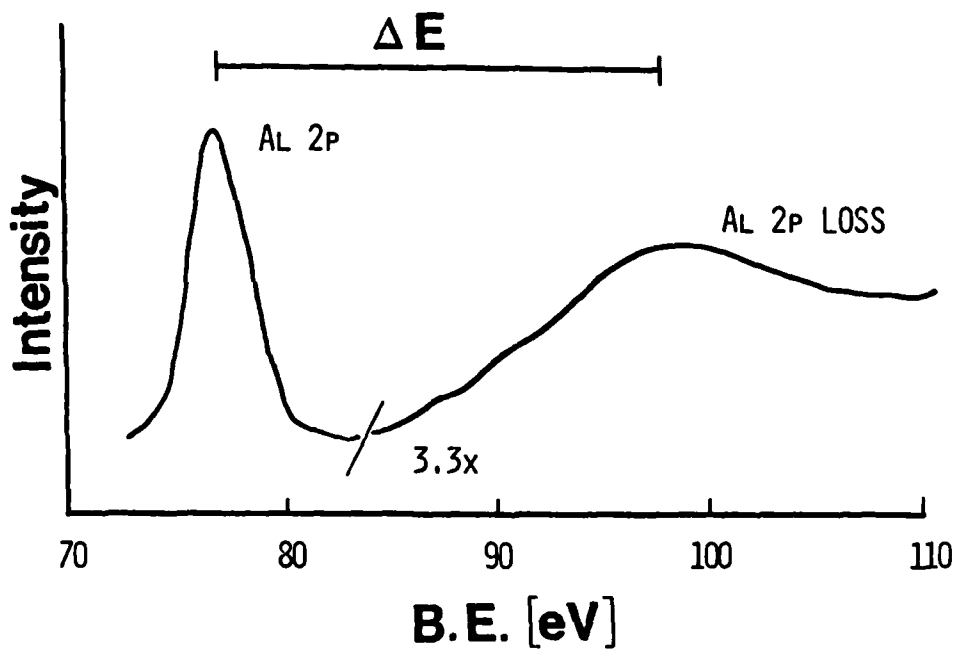


Fig. 1: A typical XPLS spectrum, associated with the Al2p photoelectron in Al-nitride.  $\Delta E$  is the separation between the principal Al2p photoelectron peak and its largest companion bulk loss peak.

for	<input checked="" type="checkbox"/>
A&I	<input type="checkbox"/>
3	<input type="checkbox"/>
ed	<input type="checkbox"/>
Availability Codes	
Dist	Avail and/or Special
A-1	

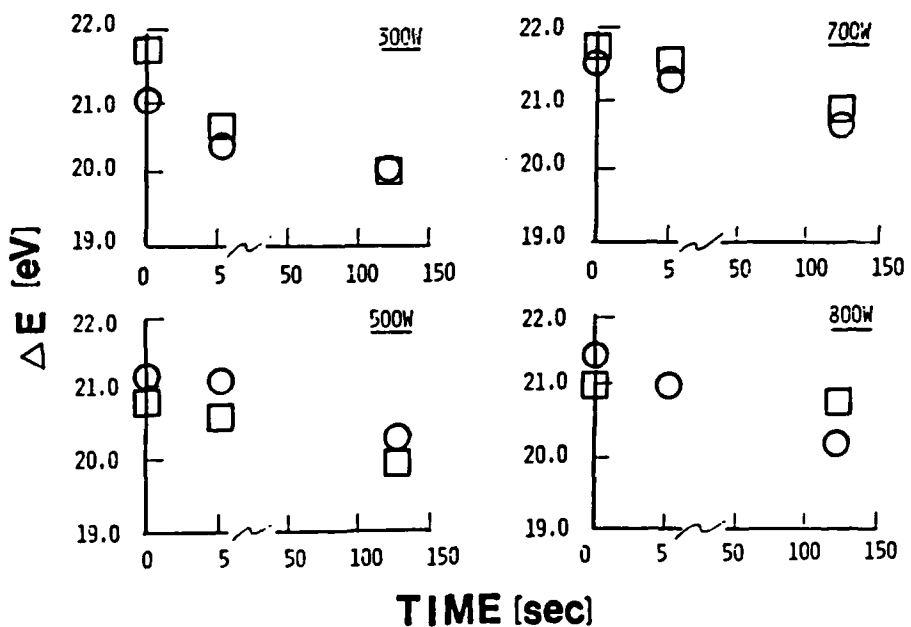


Fig. 2:  $\Delta E$  as a function of sputter etching time for sputter deposited Al-nitride films. Squares represent  $\Delta E(\text{Al}2s)$ , circles represent  $\Delta E(\text{Al}2p)$ .

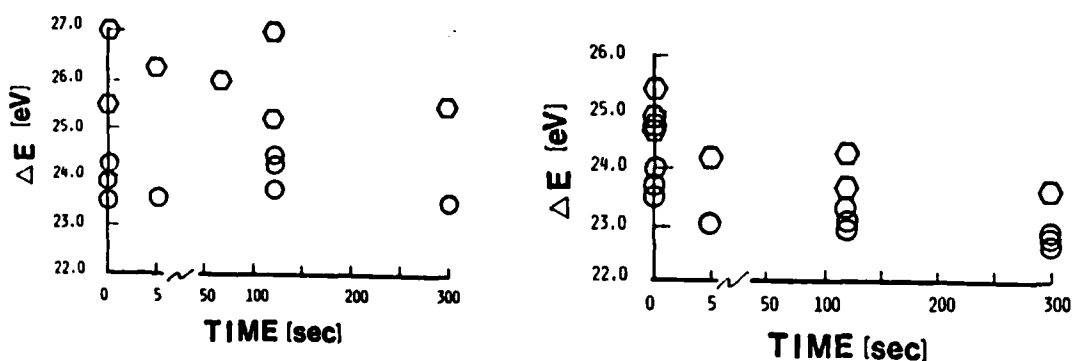


Fig. 3:  $\Delta E$  as a function of sputter etching time for (a) single crystal  $\alpha$ -alumina, (b) sputter deposited  $\alpha$ -alumina. Circles represent  $\Delta E(\text{Al}2s)$ , hexagons represent  $\Delta E(\text{Al}2p)$ .

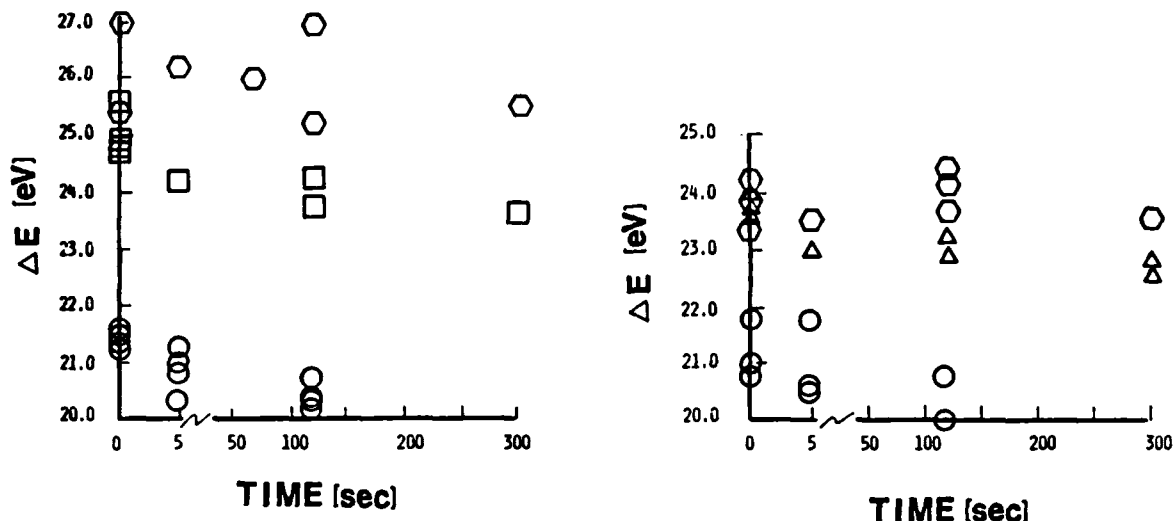


Fig. 4: (a)  $\Delta E(A12p)$  and (b)  $\Delta E(A12s)$  as a function of sputter etching time for all samples. (Hexagons- $\alpha$ -alumina; triangles and squares-a-alumina; circles-Al-nitride).

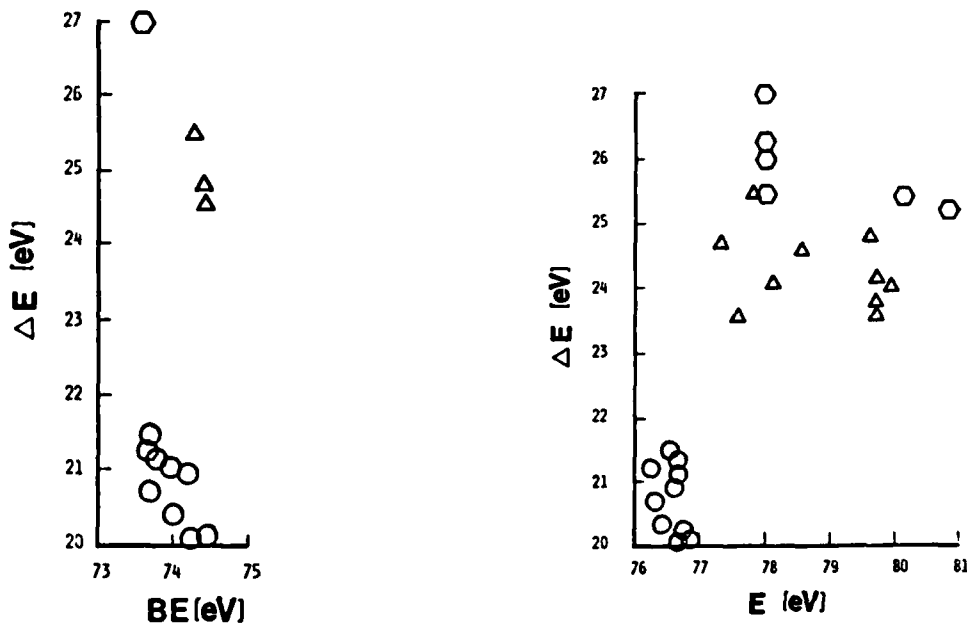


Fig. 5:  $\Delta E$  versus  $A12p$  photoelectron peak after charge referencing. (Hexagons- $\alpha$ -alumina; triangles-a-alumina; circles-Al-nitride.)

Fig. 6:  $\Delta E$  versus  $A12p$  photoelectron peak before charge referencing to C. (Hexagons- $\alpha$ -alumina; triangles-a-alumina; circles-Al-nitride.)

the Al2p principal peak energy caused by sample charging is on the order of several eV.

## DISCUSSION AND CONCLUSIONS

From the data presented above, it can be concluded that the separation of the first loss peak from its principal XPS peak for Al2p and Al2s photoelectrons differs in Al-oxides and nitrides by several eV (Figs. 2 to 4). These materials cannot be distinguished on the basis of the measured principal XPS peak energy (Fig. 5). Furthermore,  $\Delta E$  is independent of sample charging (Fig. 6). For these reasons, XPLS is a technologically useful characterization technique.

The question which remains to be addressed concerns the physical basis of the loss spectra in these wide band gap materials. In metallic Al, loss features can be attributed to plasma oscillations of the valence electrons. The value of  $\Delta E$ (Al2p) obtained by XPLS on metallic Al is 15.8 eV [5] in agreement with the value calculated using Eq. (1) for a free electron gas (FEG) [17].

Table II summarizes the range of XPLS results obtained here, as well as the calculated value of  $\Delta E$  using the FEG model. In the case of Al-nitride, it can be seen from Table II that the FEG calculation [18] yields a value within experimental error of the values for  $\Delta E$  obtained by XPLS. In addition, there is no dispersion in the values of  $\Delta E$ (Al2p) and  $\Delta E$ (Al2s). It is therefore suggested that the loss features in the XPLS spectrum of Al-nitride are plasmon in origin and  $\Delta E$  is consistent with the value calculated using a FEG model.

With respect to the aluminas, the situation is more complex. In  $\alpha$ -alumina there is a large dispersion in  $\Delta E$ (Al2p) and  $\Delta E$ (Al2s). Loss features in this material are therefore not entirely plasmon in nature. The values of  $\Delta E$ (Al2p) do not agree with FEG calculations using either 18 or 24 valence electrons/Al<sub>2</sub>O<sub>3</sub> molecule [14,15]. Agreement between  $\Delta E$ (Al2s) and FEG calculations using 18 valence electrons/Al<sub>2</sub>O<sub>3</sub> molecule may be coincidental.

TABLE II: Comparison of  $\Delta E$  Obtained by XPLS with Free Electron Gas Calculations

Material	$\Delta E$ , XPLS (eV) <sup>+</sup>	$\Delta E$ , FEG (eV)
$\alpha$ -alumina	Al2p: 25.2-27.0	24.0,* 27.9**
	Al2s: 23.0-24.5	
$\alpha$ -alumina	Al2p: 23.6-25.5	20.2,* 23.4**
	Al2s: 22.5-24.0	
Al-nitride	Al2p: 20.2-21.8	20.0
	Al2s: 19.8-21.8	

<sup>+</sup> Range of all data;  $\pm 0.4$  eV experimental error.

<sup>\*</sup> Assuming 18 valence electrons/Al<sub>2</sub>O<sub>3</sub> molecule, 02s e<sup>-</sup> not counted [14,15].

<sup>\*\*</sup> Assuming 24 valence electrons/Al<sub>2</sub>O<sub>3</sub> molecule, 02s e<sup>-</sup> counted [14,15].

In  $\alpha$ -alumina,  $\Delta E(\text{Al}2\text{p}) - \Delta E(\text{Al}2\text{s})$  dispersion has not been firmly established from the results of this study. Free electron gas calculations using 24 valence electrons/ $\text{Al}_2\text{O}_3$  molecule yield a value within experimental error of the lower end of the  $\Delta E(\text{Al}2\text{p})$  range and within the  $\Delta E(\text{Al}2\text{s})$  range of values obtained by XPLS. As in the case of  $\alpha$ -alumina, however, this agreement may be coincidental. We cannot therefore conclude that a FEG model accurately describes the loss features in aluminas. However, it is suggested that Eq. (1) be taken as the first term in a series in which successive terms account for perturbations due to non-collective behavior of part of the valence band electron population [5]. Future work will consider modification of the free electron gas model in this manner for the aluminas.

ACKNOWLEDGEMENTS: This work was supported under U.S. Army Research Office Grant No. DAAG29-84-0126. We thank M.G. Lagally for making the Auger/ESCA Laboratory at UW-Madison available for our use.

#### REFERENCES

1. C. J. G. Kubiak, C. R. Aita, F. S. Hickernell, and S. J. Joseph, Proc. Mater. Res. Soc. 47, 75 (1985).
2. J. A. Kovacich, J. Kasperkiewicz, D. Lichtman, and C. R. Aita, J. Appl. Phys. 55, 2935 (1984).
3. J. W. Gadzuk, J. Electron Spec. Rel. Phenom. 11, 335 (1977).
4. T. L. Barr, Appl. Sur. Sci. 10, 1 (1983).
5. T. L. Barr, B. Kramer, S. I. Shah, M. Ray, and J. E. Greene, Proc. Mat. Res. Soc. 47, 205 (1985).
6. D. Pines and D. Bohm, Phys. Rev. 85, 338 (1952).
7. D. Pines, Rev. Mod. Phys. 28, 184 (1956).
8. P. Norieres and D. Pines, Phys. Rev. 109, 741 (1958).
9. D. G. Welkie and M. G. Lagally, J. Vac. Sci. Technol 16, 784 (1979).
10. D. Briggs and M. P. Seah, Practical Surface Analysis by Auger and Photoelectron Spectroscopy (Wiley, New York, 1983) pp. 511-514.
11. A. F. Wells, Structural Inorganic Chemistry (Calredon, London, 1950) pp. 379-386.
12. Ibid. pp. 49, 462.
13. J. A. Thornton and J. Chin, Ceramic Bull. 56, 504 (1977).
14. W. Tews and R. Grundler, phys. stat. sol. (b), 109, 255 (1982).
15. W. Tews and R. Zimmermann, phys. stat. sol. (b) 110, 479 (1982).
16. R. G. Frieser, J. Electrochem. Soc. 113, 357 (1966).

17. O. Klemperer and J. P. G. Shepherd, *Adv. Phys.* 12, 355 (1963).
18. C. R. Aita, unpublished. (6 valence electrons/AlN molecule and 6 molecules/unit cell are assumed.)

END  
FILMED

4-86

DTIC